Available online at www.sciencedirect.com

SCIENCE DIRECT®

Journal of Electron Spectroscopy and Related Phenomena 144–147 (2005) 223–226

JOURNAL OF ELECTRON SPECTROSCOPY and Related Phenomena

www.elsevier.com/locate/elspec

Experimental and quantum–chemical studies on dissociative photoionization of c-C_2H_4S

Su-Yu Chiang[a, *], Yung-Sheng Fang[b]

[a] *National Synchrotron Radiation Research Center, 101, Hsin Ann Road, Science-Based Industrial Park, Hsinchu 30077, Taiwan*
[b] *Department of Applied Chemistry, National Chiao Tung University, 1001, Ta Hsueh Road, Hsinchu 300, Taiwan*

Abstract

The dissociative photoionization of thiirane (c-C_2H_4S) in a region ∼9–20 eV was investigated with photoionization mass spectroscopy and calculations of molecular energies with the Gaussian-3 method. An adiabatic ionization energy of 9.051 eV for c-C_2H_4S agrees with a prediction of 9.07 eV for formation of c-$C_2H_4S^+$; predictions of energies of formation of ring-opened isomers CH_3CHS^+, CH_2CHSH^+ and $CH_2SCH_2{}^+$ are 8.85, 8.91 and 9.37 eV, respectively. Major fragment ions $C_2H_3S^+$, $C_2H_2S^+$, HCS^+, H_2S^+ and $C_2H_3{}^+$ were observed with their respective appearance energies at 10.71, 13.07, 11.13, 11.96 and 12.58 eV. Based on comparison of determined appearance energies and predicted reaction energies, we established six dissociation channels $c\text{-}C_2H_4S^+ \rightarrow CH_3CS^+ + H$, $HCS^+ + CH_3$, $H_2S^+ + C_2H_2$, $C_2H_3{}^+ + HS$, $CH_2CS^+ + H_2$ and $CHCSH^+ + H_2$. Ring-opening and H migration are involved in these processes.

Keywords: c-C_2H_4S; Dissociative photoionization; Gaussian-3 method

---

1. Introduction

Thiirane (c-C_2H_4S) attracts fundamental interest in its dynamics of dissociation upon photoexcitation because its large ring strain facilitates ring-opening processes and isomerization. Photodissociation (PD) and photoionization (PI) of c-C_2H_4S also produce several important radicals and ions, and thus, offer a powerful means of obtaining information about structures and energetics of these species [1,2].

The ionization energy (IE) of c-C_2H_4S has been measured by various groups with PI [2,3], optical spectroscopy (S) [4], photoelectron spectroscopy (PES) [5,6] and the electron-impact (EI) [7] technique, but the reported IE from PI, PES and EI methods are scattered over a range 8.9–9.05 eV. Appearance energies (AE) of fragment ions $C_2H_3S^+$ and HCS^+ were determined in the gaseous phase with PI [2,3], but both AE values suffer from the effect of thermal energy. Appearance energies of fragment ions $C_2H_2S^+$, CH_2S^+, H_2S^+, S^+, $C_2H_3{}^+$, $C_2H_2{}^+$ and $CH_2{}^+$ were determined with EI [7]; AE values thus determined generally represent a qualitative indication of a dissociation threshold.

Our aim in this work is to explore dissociative photoionization of molecular-beam-cooled c-C_2H_4S with a photoionization mass spectrometer coupled to a synchrotron radiation as an ionization source and with Gaussian-3 (G3) calculations. We measured photoionization efficiency (PIE) spectra of c-C_2H_4S and various fragment ions and undertook theoretical calculations of molecular structures and energies. Comparing computed reaction energies with experimental IE and AE values, we are able to identify structures of c-$C_2H_4S^+$ and fragment ions and to propose plausible dissociation mechanisms.

2. Experiments and calculations

We performed photoionization mass-spectrometric measurements with a molecular-beam/quadrupole mass spectrometer system on the 1-m Seya-Namioka beamline at the National Synchrotron Radiation Research Center (NSRRC)

---

* Corresponding author. Tel.: +886 3 578 0281x7315; fax: +886 3 578 3813.
E-mail address: schiang@nsrrc.org.tw (S.-Y. Chiang).

0368-2048/$ – see front matter © 2005 Elsevier B.V. All rights reserved.
doi:10.1016/j.elspec.2005.01.072

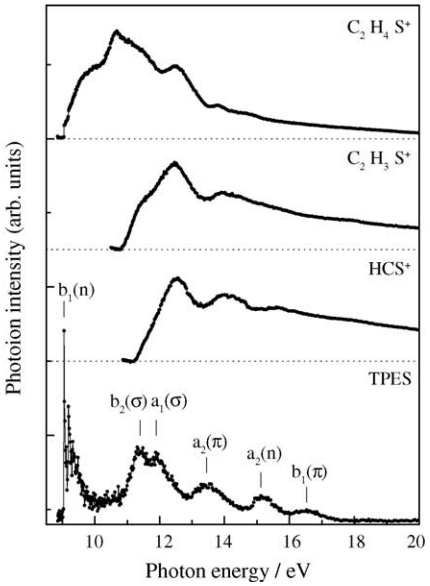

Fig. 1. Photoionization efficiency curves of *c*-C_2H_4S and two major fragment ions $C_2H_3S^+$ and HCS^+, and the threshold photoelectron spectrum of *c*-C_2H_4S in a region ∼9–20 eV.

in Taiwan. The apparatus is described in detail elsewhere [8]. Briefly, a mixture of *c*-C_2H_4S/He at a total pressure ∼300 Torr and with a seed ratio of ∼10% was expanded through a nozzle and two skimmers to form a molecular beam. The cooled *c*-C_2H_4S molecules were ionized with monochromatic VUV radiation at a right angle in the ionization chamber. Produced ions were mass-analyzed and detected with a quadrupole mass spectrometer. The PIE curves in a region ∼9–20 eV were measured and normalized with respect to the photon flux. The wavelength of the monochromator was calibrated with the photoionization spectra of Ar and He. *c*-C_2H_4S (Aldrich, ∼98%) was degassed with several freeze-pump-thaw cycles before use and was kept in an ice bath at 0 °C during experiments.

Energies of *c*-C_2H_4S, isomers of *c*-$C_2H_4S^+$ and fragment species at their equilibrium geometries were calculated with the G3 method using the Gaussian 98 program [9]. Enthalpies of formation at temperature T ($\Delta H^{\text{o}}_{\text{f},T}$) for plausible products were obtained from calculated enthalpy changes of their equations of formation and from experimental $\Delta H^{\text{o}}_{\text{f},T}$ for isolated atoms C, H and S [10]. Li et al. reported that ionization energies for several sulfur- and chlorine-containing species, and oxides predicted with the G2 method agree with experimental values typically within ±0.15 eV [11].

3. Results and discussion

In the mass spectrum of *c*-C_2H_4S excited at 60 nm, five major fragment ions, apart from sulfur isotopic species, at $m/z = 59$, 58, 45, 34 and 27 were observed, corresponding to isomeric structures of $C_2H_3S^+$, $C_2H_2S^+$, HCS^+, H_2S^+ and

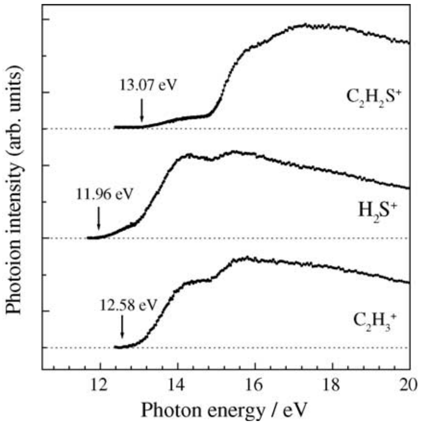

Fig. 2. Photoionization efficiency curves of $C_2H_2S^+$, H_2S^+ and $C_2H_3{}^+$ from their respective thresholds to 20 eV.

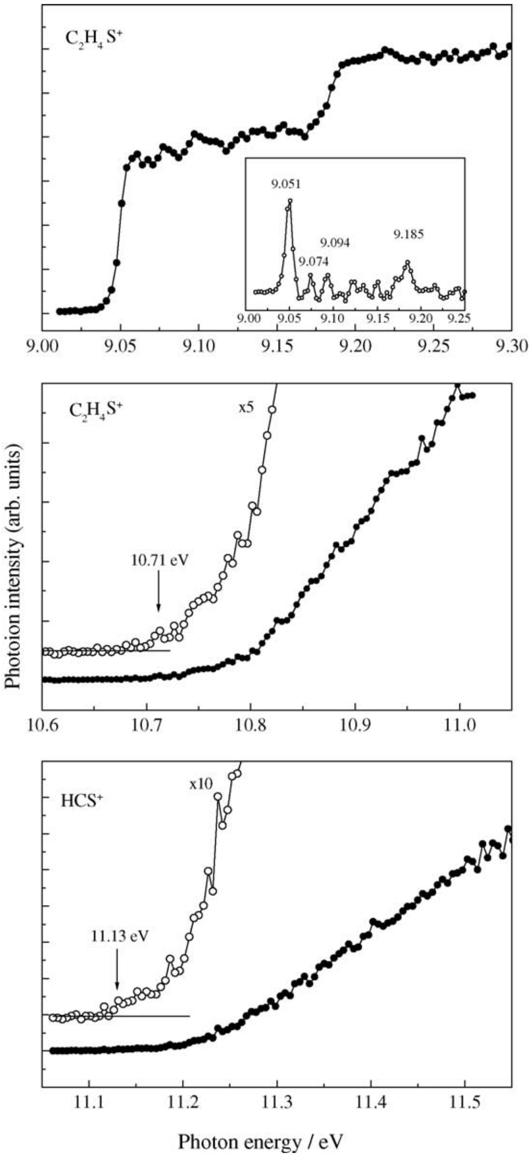

Fig. 3. Photoionization efficiency curves of *c*-$C_2H_4S^+$, $C_2H_3S^+$ and HCS^+ near the threshold region.

Table 1
Calculated total G3 energies (E_0), enthalpies (H_{298}), enthalpies of formation at 0 K ($\Delta H^o_{f,0}$) and 298 K ($\Delta H^o_{f,298}$) for species involved in dissociative photoionization of c-C_2H_4S, with symmetries and electronic states

Species	symmetry (state)	E_0 (hartree)	H_{298} (hartree)	$\Delta H^o_{f,0}$ (kcal mol^{-1})	$\Delta H^o_{f,298}$ (kcal mol^{-1})
c-C_2H_4S	C_{2v} ($^1A_1$)	−476.56145	−476.55711	21.7	19.1
CH_3CHS^+	C_s ($^2A'$)	−476.23622	−476.23109	225.8	223.7
CH_2CHSH^+	C_s ($^2A''$)	−476.23385	−476.22893	227.3	225.1
c-$C_2H_4S^+$	C_{2v} ($^2B_1$)	−476.22832	−476.22382	230.7	228.3
$CH_2SCH_2{}^+$	C_{2v} ($^2A_2$)	−476.21704	−476.21186	237.8	235.8
CH_3CS^+	C_{3v} ($^1A_1{}'$)	−475.67411	−475.66937	212.5	211.2
CH_2CSH^+	C_s ($^1A'$)	−475.63377	−475.62879	237.8	236.7
CH_2CHS^+	C_s ($^1A'$)	−475.62884	−475.62452	240.9	239.3
CH_2CHS^+	C_s ($^1A'$)	−475.58588	−475.58105	267.9	266.6
CH_2CS^+	C_{2v} ($^2B_1$)	−475.02682	−475.02203	252.7	252.4
$CHCSH^+$	C_s ($^2A''$)	−474.98173	−474.97663	281.0	280.9
HCS^+	$C_{\infty v}$ ($^1\Sigma$)	−436.36196	−436.35848	242.0	242.1
H_2S^+	C_{2v} ($^2B_1$)	−398.85461	−398.85082	236.9	236.4
HS	$C_{\infty v}$ ($^2\Sigma$)	−398.59532	−398.59201	33.6	33.8
$C_2H_3{}^+$	C_{2v} ($^1A_1$)	−77.51350	−77.50923	272.1	271.4
C_2H_2	$D_{\infty h}$ ($^1\Sigma_g{}^+$)	−77.27596	−77.27228	55.1	55.1
CH_3	D_{3h} ($^2A_2$)	−39.79330	−39.78905	34.6	34.1
H_2	$D_{\infty h}$ ($^1\Sigma_g{}^+$)	−1.16738	−1.16407	−0.5	−0.5
H	(^2S)	−0.50100	−0.49864		

$C_2H_3{}^+$, respectively; four minor fragment ions at $m/z = 57$, 46, 28 and 26 correspond to isomeric structures of C_2HS^+, CH_2S^+, $C_2H_4{}^+$ and $C_2H_2{}^+$, respectively.

Fig. 1 shows PIE curves of $C_2H_4S^+$ and major fragment ions $C_2H_3S^+$ and HCS^+ from their respective appearance onset to 20 eV; threshold photoelectron (TPE) spectrum of c-C_2H_4S is also presented to show the correlation between electronic excitation and the intensity variations of ions. According to Fig. 1, the major dissociation channel $C_2H_4S^+ \rightarrow C_2H_3S^+ + H$ requires the least energy. The similar features of intensities of $C_2H_4S^+$, $C_2H_3S^+$ and HCS^+ indicate that they are formed through similar paths. PIE curves of other major fragment ions – $C_2H_2S^+$, H_2S^+ and $C_2H_3{}^+$ – are shown in Fig. 2.

PIE curves near the threshold regions of $C_2H_4S^+$, $C_2H_3S^+$ and HCS^+, measured with steps of 0.05 nm and shown in Fig. 3(a–c), enable us to determine the AE of each fragment ion. An IE = 9.051 ± 0.003 eV for c-C_2H_4S was determined from the first distinct maximum in the first derivative of the PIE curve because of step-like features of ion signals near the threshold region. One additional distinct maximum at 9.185 eV is identified; its interval of 1089 cm^{-1} (0.135 eV) is consistent with a value of 1090 cm^{-1} for the methylene bending mode of $C_2H_4S^+$ obtained from the photoelectron spectrum [12]. From rising signals of the PIE curves near the threshold region, AE values of $C_2H_3S^+$, $C_2H_2S^+$, HCS^+, H_2S^+ and $C_2H_3{}^+$ were determined to be 10.71 ± 0.01, 13.07 ± 0.04, 11.13 ± 0.01, 11.96 ± 0.03 and 12.58 ± 0.03, respectively. As c-C_2H_4S was cooled under supersonic conditions, we ignored effects of thermal energy and collisions on our IE and AE values. The AE values for $C_2H_2S^+$, H_2S^+ and $C_2H_3{}^+$ determined with PI are reported for the first time.

Geometries of c-C_2H_4S and species involved in the dissociative photoionization were optimized at the MP2(full)/6-31G* level. The calculated G3 energies, enthalpies and standard enthalpies of formation for species pertinent to this work are listed in Table 1; symmetries and electronic states are also indicated. With the aid of these results, we calculated ionization energies of c-C_2H_4S to form isomers of c-$C_2H_4S^+$ and reaction energies of plausible channels of dissociative photoionization.

Predicted IE of c-C_2H_4S to form CH_3CHS^+, CH_2CHSH^+, c-$C_2H_4S^+$ and $CH_2SCH_2{}^+$ are 8.85, 8.91, 9.07 and 9.37 eV, respectively. The experimental IE at 9.051 ± 0.003 eV agrees satisfactorily with a prediction of 9.07 eV for formation of c-$C_2H_4S^+$ despite the energy of CH_3CHS^+ being 4.9 kcal mol^{-1} smaller than that of c-$C_2H_4S^+$; an observation of rapidly rising signals of $C_2H_4S^+$ near the ionization threshold also reflects a small structural change upon ionization. In addition, we established six dissociation channels c-$C_2H_4S^+ \rightarrow CH_3CS^+ + H$, $HCS^+ + CH_3$, $H_2S^+ + C_2H_2$, $C_2H_3{}^+ + HS$, $CH_2CS^+ + H_2$ and $CHCSH^+ + H_2$ based on comparison of determined AE values and predicted reaction energies E(G3). We discuss the dissociation mechanisms as follows.

To form $C_2H_3S^+$, loss of an H atom is the most direct way, but four isomers of $C_2H_3S^+$ are possible. Predicted E(G3) for channels c-$C_2H_4S^+ \rightarrow CH_3CS^+ + H$, $CH_2CSH^+ + H$, c-$CH_2CHS^+ + H$ and $CH_2CHS^+ + H$ are 10.52, 11.62, 11.75 and 12.92 eV, respectively. Only channel c-$C_2H_4S^+ \rightarrow CH_3CS^+ + H$ has a predicted E(G3) of 10.52 eV smaller than the experimental AE of 10.71 eV; thus, CH_3CS^+ is the most likely structure near the threshold. Holmes et al. measured an average kinetic energy release 0.15 eV for formation of $C_2H_3S^+$ [13]. A difference of 0.19 eV between experimental AE and predicted E(G3) might imply the presence of kinetic shifts and reverse activation energies for this channel. We tried to locate a transition structure for isomerization of c-$C_2H_4S^+$ to CH_3CSH^+, but a reaction barrier 1.96 eV is 0.3 eV greater than the experimental AE.

The experimental AE of 11.13 eV for channel c-$C_2H_4S^+ \rightarrow HCS^+ + CH_3$ agrees satisfactorily with the predicted E(G3) value, 11.06 eV; a small difference of 0.07 eV implies that the reverse activation energy is smaller than or near that of the products. An observation of kinetic energy release of 0.03 eV at the dissociation threshold by Butler and Baer [2] supports our proposition. The predicted structure of HCS^+ at the dissociation threshold is linear; an angular structure proposed by Butler and Baer might reflect an underestimate $\Delta H^{o}_{f,0}(HCS^+) \leq 233\,\mathrm{kcal\,mol^{-1}}$. We derive $\Delta H^{o}_{f,0}(HCS^+) = 243.5 \pm 2\,\mathrm{kcal\,mol^{-1}}$, according to experimental $AE = 11.13 \pm 0.01\,\mathrm{eV}$ ($256.7 \pm 0.3\,\mathrm{kcal\,mol^{-1}}$) and literature values $\Delta H^{o}_{f,0}(c\text{-}C_2H_4S) = 22.4 \pm 0.3\,\mathrm{kcal\,mol^{-1}}$ and $\Delta H^{o}_{f,0}(CH_3) = 35.6 \pm 0.3\,\mathrm{kcal\,mol^{-1}}$ [10]. This value agrees with the literature value 243.9 $\mathrm{kcal\,mol^{-1}}$ [14] and our predicted value of 242.0 $\mathrm{kcal\,mol^{-1}}$.

At greater ionization energies, two channels c-$C_2H_4S^+ \rightarrow H_2S^+ + C_2H_2$ and $C_2H_3{}^+ + HS$ are proposed based on comparison of their experimental AE values of 11.96 and 12.58 eV with predicted E(G3) values of 11.73 and 12.16 eV, respectively. The differences of 0.23 and 0.42 eV for both channels reflect increased excess energies involved in dissociation because of more dissociation channels in competition. To form $C_2H_2S^+$, two channels c-$C_2H_4S^+ \rightarrow CH_2CS^+ + H_2$ and $CHCSH^+ + H_2$ are energetically accessible; three-body formation channels with predicted E(G3) values greater than experimental AE are excluded. The former channel is favoured because the predicted energy of 10.00 eV is smaller than 11.23 eV for the other channel.

4. Conclusion

Dissociative photoionization of c-C_2H_4S to form fragment ions – $C_2H_3S^+$, $C_2H_2S^+$, HCS^+, H_2S^+ and $C_2H_3{}^+$ was investigated in the region ~9–20 eV. The IE of c-C_2H_4S and AE of fragment ions were derived from their respective photoionization efficiency curves. Theoretical predictions of IE for c-C_2H_4S and of reaction energies for formation of observed fragment ions and their neutral counterparts were performed with the G3 method. With the aid of the latter results, we have established six dissociative photoionization channels.

Acknowledgements

We thank NSRRC and NSC of Taiwan (contract NSC92-2113-M-213-001) for financial support.

References

[1] F. Qi, O. Sorkhabi, A.G. Suits, S.-H. Chien, W.-K. Li, J. Am. Chem. Soc. 123 (2001) 148.
[2] J.J. Butler, T. Baer, J. Am. Chem. Soc. 104 (1982) 5016.
[3] J.J. Butler, T. Baer, Org. Mass Spectrom. 18 (1983) 248.
[4] N. Basco, R.D. Morse, Chem. Phys. Lett. 20 (1973) 404.
[5] D.H. Aue, H.M. Webb, W.R. Davidson, M. Vidal, M.T. Bowers, H. Goldwhite, L.E. Vertal, J.E. Douglas, P.A. Kollman, G.L. Kenyon, J. Am. Chem. Soc. 102 (1980) 5151.
[6] A. Schweig, W. Thiel, Chem. Phys. Lett. 21 (1973) 541.
[7] E. Gallegos, R.W. Kiser, J. Phys. Chem. 65 (1961) 1177.
[8] S.-Y. Chiang, C.-I. Ma, D.-J. Shr, J. Chem. Phys. 110 (1999) 9056.
[9] M.J. Frisch, G.W. Trucks, H.B. Schlegel, G.E. Scuseria, M.A. Robb, J.R. Cheeseman, V.G. Zakrzewski, J.A. Montgomery, Jr., R.E. Stratmann, J.C. Burant, S. Dapprich, J.M. Millam, A.D. Daniels, K.N. Kudin, M.C. Strain, O. Farkas, J. Tomasi. V. Barone, M. Cossi, R. Cammi, B. Mennucci, C. Pomelli, C. Adamo, S.Clifford, J. Ochterski, G.A. Petersson, P.Y. Ayala, Q. Cui, K. Morokuma, D.K. Malick, A.D. Rabuck, K. Raghavachari, J.B. Foresman, J. Cioslowski, J.V. Oritz, A.G. Baboul, B.B. Stefanov, G. Liu, A. Liashenko, P. Piskorz, I. Komaromi, R. Gomperts, R.L. Martin, D.J. Fox, T. Keith, M.A. Al-Laham, C.Y. Peng, A. Nanayakkara, C. Gonzalez, M. Challacombe, P.M.W. Gill, B. Johnson, W Chen, M.W. Wong, J.L. Andres, C. Gonzalez, M. Head-Gordon, E.S. Replogle, J.A. Pople, GAUSSIAN 98, Revision A.7, Gaussian Inc., Pittsburgh, PA, 1998.
[10] S.G. Lias, J.E. Bartmess, J.F. Liebman, J.L. Holmes, R.D. Levin, W.G. Mallard, J. Phys. Chem. Ref. Data Suppl. 17 (1988) 1.
[11] F. Liu, L. Sheng, Y. Zhang, F. Qi, H. Gao, C. Li, Y. Zhang, S. Yu, K.-C. Lau, W.-K. Li, J. Phys. Chem. A 103 (1999) 8179.
[12] D.C. Frost, F.G. Herring, A. Katrib, C.A. McDowell, Chem. Phys. Lett. 20 (1973) 401.
[13] J.L. Holmes, P. Wolkoff, J.K. Terlouw, J. Chem. Soc. Chem. Commun. 492 (1977).
[14] B. Ruscic, J. Berkowitz, J. Chem. Phys. 98 (1993) 2568.